CrossMark

ORIGINAL ARTICLE

Xylem conductance of sweet cherry pedicels

Martin Brüggenwirth[1] · Moritz Knoche[1]

Abstract

Key message **Flow rates were quantified on detached pedicels and conductances calculated. Flow rates and conductances were independent of time and temperature, increased with the pressure applied and slightly decreased during development.**

Abstract Water uptake is thought to contribute to cracking of sweet cherry fruit. Water uptake/loss occurs not only through the fruit surface but also through the xylem and phloem of the pedicel. The objectives here were: (1) to quantify the hydraulic conductance of the pedicel xylem and (2) to identify the factors affecting pedicel xylem conductance. Using a modified pressure probe, water was forced through excised pedicels. The rates of axial flow were quantified gravimetrically by collecting water at the pedicel's distal end in a pre-weighed Eppendorf tube. Applying pressure to the proximal end of a pedicel induced a constant axial flow of water through it. The introduction of air embolisms to the xylem markedly decreased axial conductance from $1.3 \pm 0.1 \times 10^{-10}$ m^3 MPa^{-1} s^{-1} to near zero. Steam girdling had no effect on axial conductance indicating the water flows to be through the xylem, not significantly through the phloem in our ex situ arrangement. Compared with a petiole, the pedicel conductance was 50-fold lower. A cross-section of a pedicel near its distal end revealed about 10 vascular bundles that diverged from a complete ring closer to the proximal end.

Communicated by M. Zwieniecki.

✉ Moritz Knoche
moritz.knoche@obst.uni-hannover.de

[1] Fruit Science Section, Institute for Horticultural Production Systems, Leibniz University Hannover, Herrenhäuser Straße 2, 30419 Hannover, Germany

Conductance estimates from the numbers and sizes of xylem vessels using Hagen–Poiseuille's law exceed those determined experimentally by about three to fourfold. Conductance of pedicels decreased slightly in developing fruit and then remained about constant until maturity. Surprisingly, there was no significant effect of temperature on conductance. The conductance estimates may be used to model xylem water flows through the pedicel.

Keywords *Prunus avium* · Hydraulic conductivity · Flow · Pressure probe · Water

Introduction

Fruit cracking limits sweet cherry production in almost all areas of the world in which they are grown and leads to significant, sometimes catastrophic, economic loss (Christensen 1996). Water uptake by the fruit is thought to be a major cause of cracking. Water enters and leaves a fruit along several pathways: through the skin surface and also through the pedicel. Because of the phenomenological link between the occurrence of rain and the incidence of ('rain') cracking, studies have traditionally focussed on the osmotic uptake of water through the skin (Beyer and Knoche 2002; Beyer et al. 2002, 2005; Weichert and Knoche 2006) and, less so, on the reduction of transpiration through a partially wetted skin (Knoche et al. 2000, 2001). In comparison, water movements into and out of the fruit through the pedicel's vascular system have received much less attention. Hovland and Sekse (2004a, b) used a potometric approach to determine (xylem) vascular uptake by detached fruit. In potometry, a fruit with its pedicel is detached from the tree by cutting under water to avoid air embolism and subsequently mounted in a glass capillary filled with water. As water is drawn into the fruit,

the air:water meniscus in the capillary moves and this movement is recorded with respect to time (Hovland and Sekse 2004a). Potometers quantify the flow of xylem water driven by the pressure potential difference between the outside world and the inside of the fruit (the fruit apoplast). The latter pressure deficit is usually assumed to arise as a result of fruit transpiration and—if present—from an osmotic gradient (Knoche et al. 2015). Measham et al. (2010) employed a heat pulse sensor to study vascular transport in the pedicels of fruit that remained attached to the tree. In this technique, the net flow through the xylem and phloem is monitored by following the propagation of a heat pulse along the pedicel, which travels in the dominant direction of sap flow. However, in many fruits, the xylem and phloem flows are in opposite directions in day time, and in the same direction only at night, this makes interpretation of such experiments difficult (Lang 1990; Morandi et al. 2010). Separation of the xylem and phloem flow components is not possible without further manipulation such as disabling the phloem by steam girdling. Because the driving forces are unknown, hydraulic conductances of the pedicels are difficult to calculate. In grapes, Tyerman et al. (2004) employed a pressure probe to investigate hydraulic flow in the xylem under controlled conditions. This technique allows application of a pressure and the quantification of a resulting flow. From these data, the hydraulic conductance, i.e. the flow per unit pressure and time, may be calculated which is useful for understanding water relations of the fruit influenced by the pedicel. To our knowledge, such information is not yet available for sweet cherry.

The objectives of our study were: (1) to develop a protocol for quantifying xylem hydraulic conductance in sweet cherry pedicels using a pressure probe and (2) to identify factors affecting it.

Materials and methods

Plant material

Sweet cherries (*Prunus avium* L.) 'Brooks', 'Dönissens Gelbe Knorpelkirsche', 'Flamengo Srim', 'Gill Peck', 'Hedelfinger', 'Kordia', 'Oktavia', 'Regina', 'Sam', 'Schneiders Späte Knorpel', 'Staccato' and 'Sweetheart' were harvested at commercial maturity from the horticultural experiment station of the Leibniz University in Ruthe (lat. 52°14′N, long. O 9°49′E) or from the Herrenhausen campus in Hannover (lat. 52°23′N, long. O 9°42′E). All trees were grafted on Gisela 5 rootstocks (*Prunus cerasus* L. X *Prunus canescens* Bois) and grown under a rain shelter. Water was supplied via drip irrigation. The drip irrigation was operated for 2-h intervals (corresponding to about 15 mm of precipitation) as needed based on visual inspection of the soil

moisture of the top soil (<20 cm). Leaves from 'Regina' were obtained from the same trees. Fruit were free of visual defects and uniform in size and colour. To avoid air embolism, fruit and leaves were submerged in water and then detached from the tree. Pedicels and petioles remained submerged while they were carried to the laboratory (a short walk) and processed. All experiments were conducted within 0.5 h of detachment from the tree.

General procedure for determining pedicel conductance

Unless otherwise stated, pedicels were trimmed to 35 mm length by re-cutting the proximal end under water using a razor blade. The proximal end was then inserted in a water-filled ethylene-tetrafluoroethylene tube (ETFE; inner diam. 1.6 mm) and the tube:pedicel juncture sealed using cyanoacrylate adhesive (Loctite 406; Henkel Loctite, München, Germany) and activator (Toolcraft Aktivator-Spray; Conrad Electronic SE, Hirschau, Germany). The water was deionised, filtered (Rotalibo®-syringe filter, CME, 0.22 µm pore diameter; Carl Roth, Karlsruhe, Germany) and degassed. Subsequently, the fruit was detached from the distal end of the pedicel and the free end of the ETFE tube was similarly sealed into a glass capillary (inner diam. 0.3 mm, length 100 mm) attached to a modified pressure probe (Fig. 1a; for details see Steudle 1993). Pedicels were carefully wrapped in wet tissue paper to minimise transpiration. The pressure probe consisted of a chamber filled with silicone oil (Wacker AS 4; Wacker Chemie, München, Germany) and equipped with a pressure sensor (26PCGFA6D; Honeywell, Golden Valley, MN, USA). The glass capillary was attached to the chamber such that one end of the capillary was in contact with the silicone oil in the chamber and the other end with the water in the ETFE tube. The whole was so arranged that the silicone oil:water meniscus resided in the glass capillary where it could be observed using a horizontal binocular microscope (M80; Leica Microsystems, Wetzlar, Germany). By driving a motorised piston into the silicone oil-filled chamber, oil was displaced, which pressurised the water in the capillary and forced it to flow into the pedicel. Unless otherwise stated, pressure was gradually increased to 10 kPa and then held constant for about 5 min. The water flow rate into the pedicel was quantified by monitoring the movement with time of the oil:water meniscus in the glass capillary using the horizontal binocular microscope. In preliminary experiments, water droplets appeared on the pedicel surface towards the proximal (high pressure) end, indicating a radial flow component. Because the movement of the meniscus records the total inflow into the pedicel, this radial flow component will result in a corresponding overestimate of the axial flow which it is desired to measure. A procedure was then developed to quantify just the axial flow component by recording the water
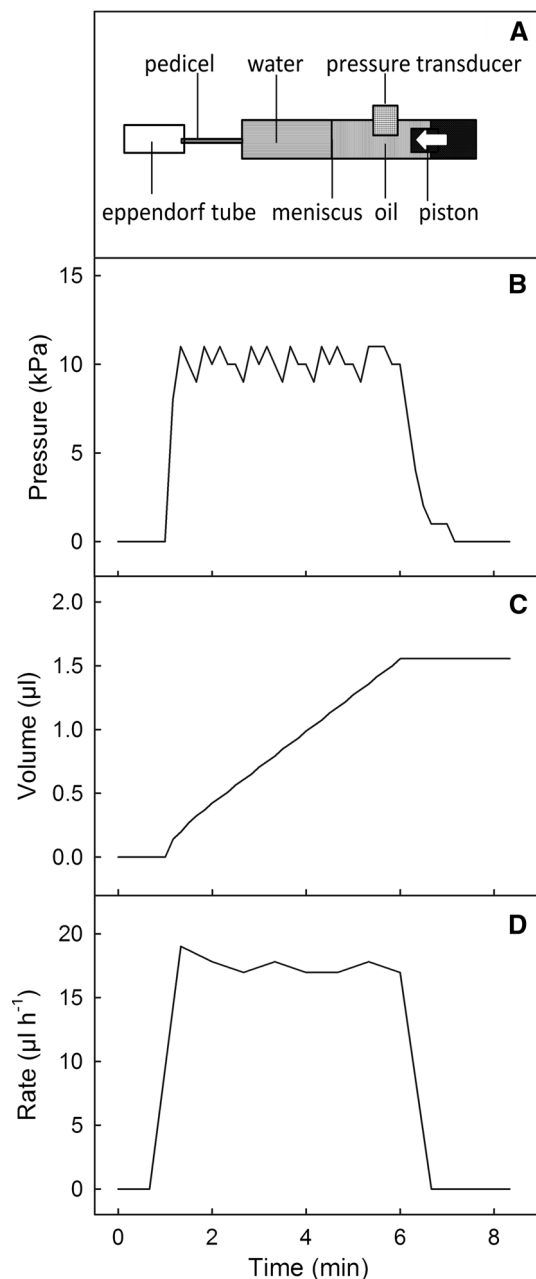
Fig. 1 a Schematic diagram of the pressure probe setup used to quantify hydraulic conductance in sweet cherry pedicels. Pressure is generated by driving a piston into a chamber filled with silicone oil. Total water flow is recorded by following the movement of the water:oil meniscus using a horizontal microscope. Total flow comprises a radial flow component that exits via the pedicel surface and an axial flow component which passes along the xylem to the cut surface of the distal end of the pedicel. The axial flow is quantified gravimetrically by collecting water emerging from the distal end in an Eppendorf tube (for details see in "Materials and methods"). **b, c, d** Representative time course of change in pressure (**b**), and its effect on cumulative water inflow into the pedicel (**c**) and on the rate of inflow during a typical test (**d**)

outflow from the distal end of the pedicel. To do this, the distal end was inserted through a 2-mm-diameter hole in a rubber septum sealing the lid of a pre-weighed Eppendorf tube filled with tissue paper. The septum was necessary to prevent water loss by evaporation. Axial outflow from the pedicel was quantified gravimetrically by weighing the Eppendorf tube before and after pressurising the chamber. From the axial flow rate, the hydraulic conductance (k_h, m^3 s^{-1} MPa^{-1}) was calculated according to Eq. 1, where ΔV is the volume (m^3) of water collecting in the Eppendorf tube during the time period Δt (s) at a pressure difference ΔP (MPa).

$$k_h = \frac{\Delta V}{\Delta P \cdot \Delta t}. \tag{1}$$

Experiments

The time course of water inflow to the proximal end of the pedicel was quantified frequently from the incremental movements of the oil:water meniscus in the glass capillary. The water outflow from the distal end of the pedicel was quantified intermittently (every 5 min) from the amount (weight) of water collecting in the Eppendorf tube. The difference between the water inflow (total) and water outflow (axial) rates estimates the radial flow component lost through the pedicel surface. To visualise and localise the radial flow, aqueous solutions of fuchsin (0.01 %) or calcofluor white (0.1 %) were forced through the pedicel using the pressure probe. Images of droplets of dye solution forming on the pedicel surface were taken using a digital camera (Canon EOS 550D, lens EFS 60 mm, f/2.8 Macro USM; Canon Deutschland, Germany). To localise calcofluor white at the tissue level, cross- and longitudinal sections were prepared using a razor blade and these were viewed under a fluorescence microscope (BX-60; Olympus Europa, Hamburg, Germany; camera: Olympus DP71, Olympus Europa; filters U-MWU 330–385 nm excitation, ≥420 nm emission).

The effect of different applied pressures on the magnitudes of the total, axial and radial flows was investigated in 'Regina' pedicels. Flows were measured (total and axial) and calculated (radial) at pressures from 0 kPa to 20 kPa. In an additional experiment, the pedicel was sealed at its distal end. Under these conditions, the water inflow was equal to the radial flow (the outflow having been stopped).

The consequences of air embolism of the xylem vessels were studied in 'Oktavia' using a repeated-measures design. A pedicel was mounted in the pressure probe and the axial flow rate determined as described above. The pedicel was then removed from the ETFE tube and air embolism induced by allowing it to transpire under ambient laboratory

conditions for 10 min without a water supply. The (presumed) embolised pedicel was then re-mounted as described above, and its axial hydraulic conductance re-measured. Non-embolised pedicels served as controls.

The vascular system (xylem or phloem) that accounts for the axial flow was identified by quantifying pedicel conductance before and after steam girdling of 'Brooks' pedicels. The steam was applied using a modified steam generator for 20 s (width of girdle ∼5 mm; Kärcher SC952; Alfred Kärcher, Winnenden, Germany). Non-girdled pedicels were used as controls.

The effect of sealing the pedicel surface to prevent radial flow was studied in 'Regina'. Flow rates were first established under standard conditions as described above. Next, the entire pedicel surface was sealed using silicone rubber (744 Silicone Adhesive/Sealant; Dow Corning, Midland, MI, USA) and the inflow rate was re-measured.

Flow rates through the pedicels of fruits and the petioles of leaves were compared in 'Regina' using the procedure described above. Conductances were first determined for pedicels and petioles from pairs of measurements of axial flow rate and pressure gradient and these were compared to conductances calculated from the mean numbers and diameters of xylem vessels using the Hagen–Poiseuille law (Nobel 1999). Diameters of xylem vessels were quantified in cross-sections in the mid-portion of pedicels and petioles by light microscopy (BX-60 and DP 71 Olympus Europa) and image analysis (Cell-P, Olympus Soft Imaging Solution, Münster, Germany).

The effect of pedicel length on vascular flow and conductivity (K_h) was studied in 'Regina' using a repeated-measures design. Conductivity was first established for a 45 mm length of pedicel. The pedicel was then shortened, stepwise, to a minimum length of 15 mm by periodically cutting 10 mm lengths from the distal end using a razor blade. Conductivity was re-measured after each cut. Hydraulic conductivity (K_h, $m^4 s^{-1} MPa^{-1}$) was calculated from hydraulic conductance by multiplying by the pedicel length l (m).

$$K_h = k_h \times l. \tag{2}$$

The effect of temperature on pedicel conductance was investigated in 'Regina'. Flow rates were measured at 10, 20, 28 and 35 °C and conductances calculated.

Data analysis

Unless otherwise stated, data are presented as means and standard errors of the means (SEM) of 10 replicates. Data were subjected to analysis of variance and linear regression analysis. Mean comparisons were made using Tukey's Studentised range test ($P \leq 0.05$, package multcomp 1.2–12, procedure glht, R 2.13.1; R Foundation for Statistical Computing, Wien, Austria) and a t test ($P \leq 0.05$, R

2.13.1). The significance of coefficients of correlation (r) and determination (r^2) at $P < 0.05$, 0.01 and 0.001 is indicated by *, ** and ***, respectively.

Results

The application of a steady pressure using the pressure probe resulted in a continuous increase in the cumulative flow along the pedicel. At constant pressure, the cumulative flow as indexed by the movement of the meniscus, increased linearly with time indicating that the flow rate was constant (Fig. 1b–d).

In the initial experiments, droplets were observed to form on the pedicel surface predominantly in the proximal portion (Fig. 2a, b). The frequency and size of the droplets decreased as the distance from the pressure probe increased and (presumably) as the xylem hydrostatic pressure declined towards atmospheric. The droplets would seem to indicate a radial flow from the xylem to the pedicel surface that contributes to the inflow measurement as quantified by the movement of the oil:water meniscus in the capillary. The radial flow is likely an artefact of the (positive pressure) experimental method with only the axial flow component being physiologically meaningful. The radial flow component was quantified by subtracting the outflow (measured by weight of Eppendorf tube) from the inflow (measured by movement of the oil:water meniscus). The outflow is assumed to measure the axial flow component.

Time course studies established that the cumulative axial flow increased linearly with time as did the cumulative total flow and the cumulative radial flow (Fig. 3).

Increasing the pressure increased the total, the axial and the radial flows linearly (Fig. 4a). There was no difference between the two measurements of radial flow—, i.e. that recorded after sealing the pedicel end and that obtained by subtracting the axial outflow from the total inflow (Fig. 5a). On average, across all pressures, the radial and axial paths accounted for 66.1 ± 1.7 and 33.9 ± 1.7 % of the total flow, respectively. The pedicel conductance calculated for axial flow was constant and independent of the applied pressure (Fig. 4b).

Sealing the pedicel surface to stop the radial flow increased the axial conductance to almost the same amount as the total conductance (Table 1).

Induction of (presumed) air embolisms in the xylem markedly decreased the pedicel's axial conductance from $1.3 \pm 0.1 \times 10^{-10} m^3 MPa^{-1} s^{-1}$ to nearly zero (Table 2). In the non-embolised controls, there was no detectable change in conductance when flows were re-measured on the same pedicels (i.e. after remounting but in the absence of embolism by air drying).
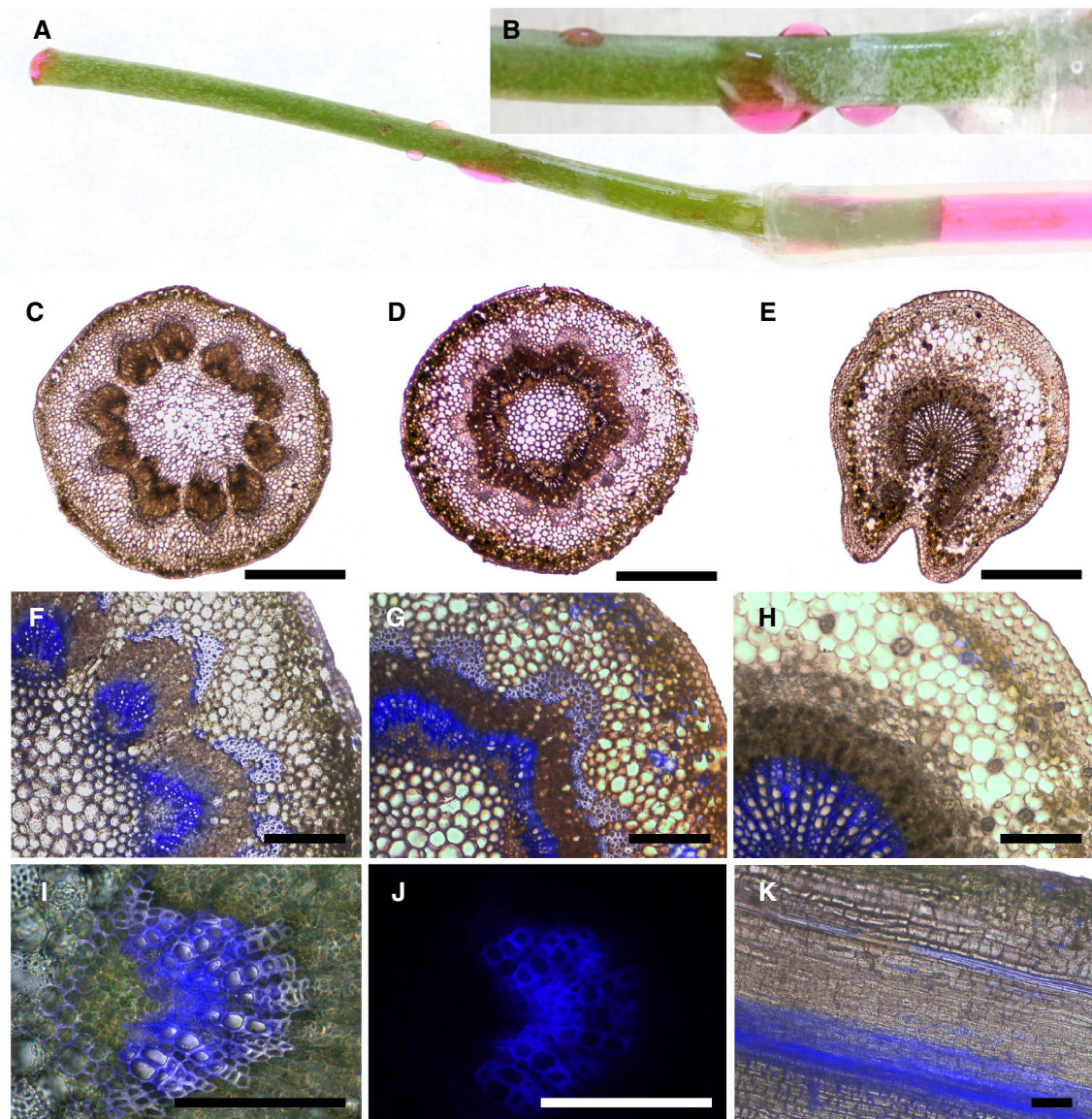
Fig. 2 **a** Macroscopic view of a pedicel mounted in a plastic (ETFE) tube, the other end of which was connected to the pressure probe via a glass capillary. Upon pressurising, dye infiltration occurred and droplets formed on the pedicel surface indicating a component of radial flow. **b** Detailed view of droplets on the pedicel surface. **c**, **d** Cross-sections of distal (**c**) and proximal (**d**) ends of a pedicel. *Bars* 1 mm. **e** Cross-section of a leaf petiole. *Bars* 1 mm. **f–h** Cross-section of a fruit pedicel in distal (**f**) and proximal regions (**g**) and cross-section of leaf petiole in the centre region (**h**). *Bar* 0.2 mm. **i–k** Cross-section (**i**, **j**) and longitudinal section (**k**) through a vessels under incident (**i**, **k**) and fluorescent lighting (**j**). *Bars* 0.2 mm. The blue fluorescence indicates staining of cell walls by the dye calcofluor white

Steam girdling had no effect on pedicel axial conductance (Table 3).

Cross-sections of the proximal region of the pedicels of mature fruits showed a complete ring of vascular tissue, but this ring separated towards the distal region to form about 10 distinct vascular bundles (Fig. 2c, d). In contrast, the vessels of the petioles were arranged in a horseshoe (Fig. 2e). When operating the pressure probe using 0.1 % aqueous calcofluor white, the vessels were stained (Fig. 3i–k). In the proximal region of the pedicel, some staining of sclerenchyma fibres and of the parenchyma also occurred (Fig. 2f–h). Compared to petioles, pedicels have fewer and smaller xylem vessels (Table 4). Consistent with the lower numbers and smaller diameters of the vessels of pedicels as compared to petioles, was a 50-fold lower conductance of the pedicels. Interestingly, the conductance calculated from the numbers and diameters of vessels using Hagen–Poiseuille's law exceeded the experimentally determined conductances by about three- to fourfold for both, pedicels and petioles (Table 4).

The axial flow through the pedicel increased as pedicel length decreased (Fig. 5a). The conductivity was lowest for the longer pedicels, but increased as pedicel length
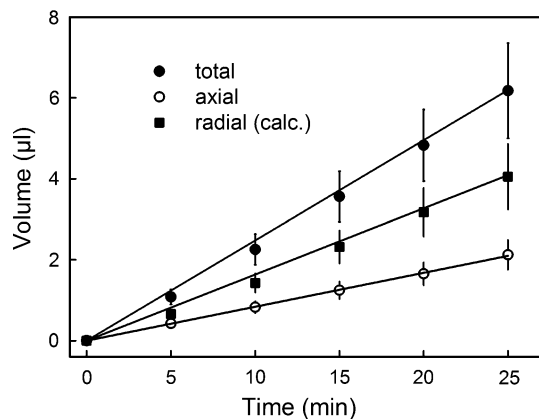
Fig. 3 Time course of cumulative water volume injected into the pedicel, the cumulative volume collected from the distal end of the pedicel ('axial') and that appearing on the pedicel surface ('radial'). The radial flow to the surface was calculated by subtracting the axial outflow from the total inflow. Total flow was quantified by recording movement of the oil:water meniscus in the capillary, and thus the water flow entering the proximal end of the pedicel. Axial flow was quantified gravimetrically by recording the water exiting the distal end of the pedicel using a pre-weighed Eppendorf tube ($n = 10$)
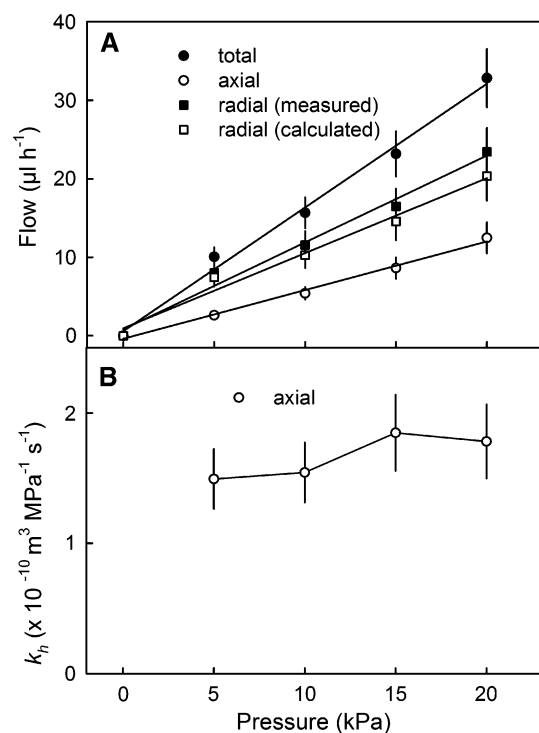

Fig. 4 a Relationship between pressure and flow rates along the different pathways in a sweet cherry fruit pedicel. The total flow refers to the sum of the axial flow plus the radial flow through to the pedicel surface. Total flow was determined from the movement of the oil:water meniscus in the capillary, the axial flow as the amount of water collecting at the distal end in a pre-weighed Eppendorf tube. Radial flows were calculated by subtracting the axial flow from the total flow ('radial calculated') or measured as the total flow through a pedicel whose distal end had been sealed ('radial measured'). b Relationship between axial conductance (k_h) and pressure ($n = 10$)
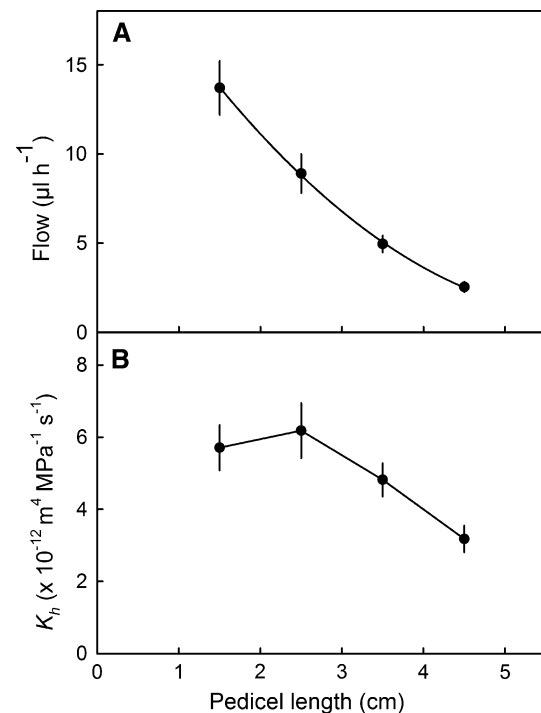

Fig. 5 Relationship between flow rate and length (a) and conductivity (K_h) and length (b) of 'Regina' pedicels ($n = 10$)

decreased (Fig. 5). Conductivity also remained constant with time.

There was little difference in pedicel conductance between different cultivars (Table 5). The only exception was 'Staccato', which had a significantly higher conductance than 'Flamengo Srim' (Table 5).

Fruit mass increased with time sigmoidally representing stages II and III of development. Conductance of pedicels during stage II decreased slightly but it remained fairly constant through stage III (Fig. 6).

There was no significant effect of temperature on pedicel conductance (Fig. 7).

Discussion

Our results demonstrate: (1) that apoplastic (xylem) sap flow and conductance in the pedicel of sweet cherry fruit can be determined reproducibly using a pressure probe in conjunction with the test protocol described herein; (2) that conductance of the fruit pedicel is much lower than that of the leaf petiole—the conductance value is also significantly lower than that predicted based on the numbers and diameters of the xylem vessel elements using Hagen Poiseuille's law, and (3) that conductance depends to some extent on pedicel length and the stage of development, but not on temperature.

Table 1 The effect on the conductance of 'Regina' sweet cherry pedicels of sealing the pedicel surface with silicone rubber

Treatment	Conductance ($\times 10^{-10}$ m^3 MPa^{-1} s^{-1})					
	Axial			Total		
	Before	After	Ratio	Before	After	Ratio
Control	1.5 ± 0.0a	1.4 ± 0.0b	1.2 ± 0.4b	6.6 ± 0.1a	6.7 ± 0.1a	1.0 ± 0.1a
Sealed	1.4 ± 0.0a	5.3 ± 0.1a	0.3 ± 0.1a	6.5 ± 0.1a	6.3 ± 0.1a	1.0 ± 0.1a

Axial conductance was calculated from gravimetric measurements of the water outflow from the distal cut surface of the pedicel, while total conductance (the axial plus the radial components) was calculated from potometric measurements of the water inflow to the proximal cut surface of the pedicel

Data are mean ± SE ($n = 10$). Mean separation within columns by Tukey's Studentised range test ($P < 0.05$)

Table 2 Effect of putative air embolism on pedicel conductance of 'Oktavia' sweet cherries

Treatment	Conductance		
	($\times 10^{-10}$ m^3 MPa^{-1} s^{-1})		
	Before	After	Ratio
Control	1.3 ± 0.0a	1.3 ± 0.0a	1.0 ± 0.1a
Cavitated	1.3 ± 0.1a	0.1 ± 0.0b	20.1 ± 6.9b

Air embolism was induced by allowing pedicels to transpire for 10 min under ambient laboratory conditions in the absence of a water supply

Data are mean ± SE ($n = 10$). Mean separation within columns by Tukey's Studentised range test ($P < 0.05$)

Table 3 Effect of steam girdling on pedicel conductance of 'Brooks' sweet cherries

Treatment	Conductance		
	($\times 10^{-10}$ m^3 MPa^{-1} s^{-1})		
	Before	After	Ratio
Control	1.0 ± 0.1a	1.0 ± 0.1a	1.0 ± 0.1a
Girdling	0.9 ± 0.1a	1.0 ± 0.1a	0.9 ± 0.1a

A fine jet of steam was directed onto a 5-mm portion of the pedicel for 20 s

Data are mean ± SE ($n = 10$). Mean separation within columns by Tukey's Studentised range test ($P < 0.05$)

Quantifying pedicel conductance using a pressure probe

Unlike the rachis of grape (Tyerman et al. 2004) exposing pedicels of sweet cherry to pressurised water at one end resulted in both axial and radial flows. The latter appeared as droplets on the pedicel surface with minimum time delay following the application of pressure. Because of the radial flow component, a meaningful measurement of axial flow in the cherry pedicel could be obtained only by measuring the water outflow rate from the distal end of the pedicel (not by measuring the water inflow rate at the proximal end). The axial flow probably occurred predominantly in the xylem. First, because (putative) air embolism of the xylem substantially stopped all flow (Table 2). Second, steam girdling (which kills the sieve tubes) had no significant effect on the flow rates measured (Table 3). Third, staining appeared almost exclusively in the xylem vessels when pedicels were pressure infiltrated with a calcofluor white dye solution (Fig. 2).

The radial flows occurred through the intercellular spaces in the parenchyma of the pedicels (Fig. 2d, g). These spaces became hydraulically connected to the pressure probe when mounting the cut end of the pedicel in the ETFE tube. Because the pedicel surface is stomatous (Athoo et al. 2015), water exited the pedicel probably through open stomata. The radial flow obeyed Darcy's law, which describes a linear relationship between the flow rate through a porous matrix and the pressure gradient over a given length. First, cumulative flow was a linear function of time and of applied pressure (Figs. 3a, 4a). Second, radial flow decreased along the pedicel as indexed by a decrease in the size of the droplets forming on the pedicel surface (Fig. 2a). Over the pressure range investigated, there was essentially no detectable radial flow beyond about 10 mm of the proximal pedicel end.

Comparing conductances of fruit pedicel, leaf petiole and published data for other crops

The 50-fold smaller conductance of fruit pedicels compared to the leaf petioles was due to the relatively smaller size and smaller number of xylem vessels in pedicels compared to petioles (Table 1). This difference is not surprising considering the much larger amounts of water transpired by leaves compared with fruits (Clearwater et al. 2012). Fruits typically have a much lower volume to surface area ratio and the fruit skin usually has a much lower density of stomata (Knoche et al. 2000; Knoche et al. 2001). Most often fruit stomata are non-functional and become lenticellular (Peschel et al. 2003).

Table 4 Numbers and diameters of xylem vessels, and calculated and measured conductance of 'Regina' fruit pedicels and leaf petioles

Organ	Xylem		Conductance	
	Elements (no.)	Diameter (μm)	Calculated (× 10^{-10} m³ MPa⁻¹ s⁻¹)	Measured (x 10^{-10} m³ MPa⁻¹ s⁻¹)
Pedicel	230.3 ± 5.2a	6.9 ± 0.1a	4.8 ± 0.2a	1.3 ± 0.1a
Petiole	306.3 ± 21.9b	16.5 ± 0.6b	244.6 ± 20.5b	53.8 ± 7.7b

Conductance was calculated from mean vessel diameter using the Hagen–Poiseuille law and compared to the conductance measured using the pressure probe

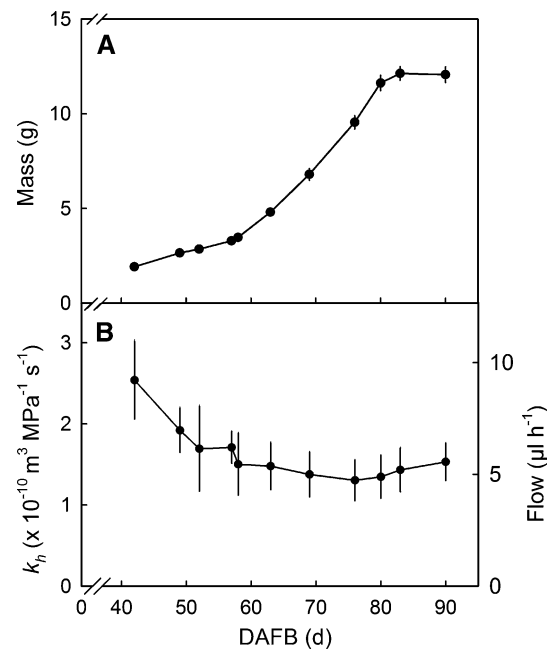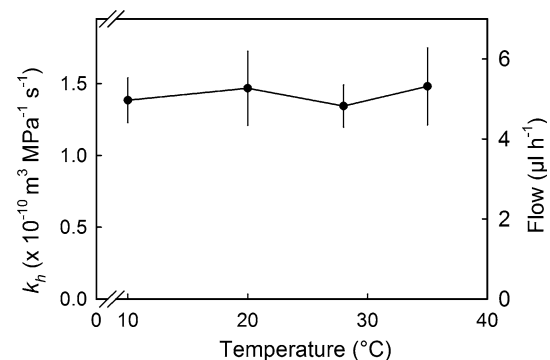Data are mean ± SE ($n = 10$). Mean separation within columns by Tukey's Studentised range test ($P < 0.05$)

Table 5 Conductances of pedicels of different cultivars of sweet cherry at maturity

Cultivar	Conductance (× 10^{-10} m³ MPa⁻¹ s⁻¹)
Dönissens Gelbe Knorpelkirsche	1.5 ± 0.1ab
Flamengo Srim	1.3 ± 0.1b
Gill Peck	1.5 ± 0.2ab
Hedelfinger	1.6 ± 0.2ab
Kordia	1.6 ± 0.2ab
Regina	1.5 ± 0.1ab
Sam	1.7 ± 0.1ab
Schneiders Späte Knorpel	1.7 ± 0.1ab
Staccato	2.0 ± 0.2a
Sweetheart	1.6 ± 0.1ab
Grand mean	1.6 ± 0.1ab

Pedicel length was standardised to 35 mm by cutting off the surplus distal portion of the pedicel

Data are mean ± SE ($n = 10$). Mean separation by Tukey's Studentised range test ($P < 0.05$)

Fig. 6 Developmental time course of conductance (k_h) from pedicels of 'Regina' sweet cherries. *Inset* mass of fruit as a function of time ($n = 10$)

Fig. 7 Conductance (k_h) of 'Regina' sweet cherry pedicels as a function of temperature ($n = 10$)

Interestingly, estimated conductance values based on the numbers and diameters of xylem vessels using Hagen–Poiseuille's law consistently exceeded the measured values by about three- to fourfold (Table 1). Several factors may be involved. First, cross-sectional areas per pedicel were measured in only one position. Any terminal narrowing of vessels would contribute to low hydraulic conductance (bottleneck), but may pass undetected in a cross-section inspected by microscopy (Drazeta et al. 2004). Second, perforation plates separating adjacent vessels reduce the hydraulically relevant vessel diameter, and are also not necessarily detected in microscopic inspections of cross-sections (Sperry et al. 2005). In the sweet cherry fruit pedicel, element lengths average ∼0.52 ± 0.03 mm (Brüggenwirth unpublished data), so the likelihood of viewing any constrictions due to the presence of perforation plates in an approximately 50-μm-thick cross-section is low. Third, not all vessels present necessarily contribute to flow. Some early formed vessels (protoxylem) in pedicels and petioles may become dysfunctional through excessive stretching during growth and thereby reduce the cross-sectional area for water movement, but again may pass undetected in microscopy. Also blockage of the

vessels due to embolism prior detachment from the tree could be possible (Sperry et al. 1988).

Comparing our estimates of the hydraulic conductance of sweet cherry to published data is somewhat limited. Information on driving forces and/or geometry of the pedicel/rachis is frequently not available (Hovland and Sekse 2004a; Measham et al. 2010). This would be required to express measured flow rates as conductances and conductivities. Nevertheless, the following comparisons may be made. In our system, flow rates among several cultivars averaged $5.5 \pm 0.5\ \mu l\ h^{-1}$ for a standard 35 mm length of pedicel with a 10-kPa pressure difference across its ends (Table 5). This rate is similar to those ($5.1\ \mu l\ h^{-1}$) determined using a potometer and a 20 mm length of pedicel attached to a non-transpiring fruit (Hovland and Sekse 2004a). Unfortunately, the driving force in the latter study is unknown. Non-transpiring fruits attached to a pressure probe develop a negative pressure of -30.3 ± 2.0 kPa (Knoche et al. 2015). Assuming that the driving force in the study by Hovland and Sekse (2004a) was similar to that reported by Knoche et al. (2015), pedicel conductances must have been of the same order of magnitude as those observed in our study.

Flow rates reported by Measham et al. (2010) averaged $0.2\ \mu l\ h^{-1}$ and were very much lower than those quantified by Hovland and Sekse (2004a). This is somewhat surprising at first sight since the heat pulse technique quantifies a net flow that represents the sum of the phloem plus the xylem flows. However, it is important to note that the driving forces are unknown and depending on the water potential in the tree (and thus the time of day or night), significant back flow from a fruit into the tree or vine may occur (Tyerman et al. 2004).

Tyerman et al. (2004) and Choat et al. (2009) focused on localising and quantifying internal resistances in the grape berry and its rachis. Grape has a branched rachis with short pedicels supplying individual berries as compared to the sweet cherry. When down scaling our conductance estimates from the standard pedicel length of 35 mm to a hypothetical length of 15 mm and then taking the inverse (for converting into a resistance), resistance estimates somewhat lower than those published for ripe 'Chardonnay' grapes (approx. 20×10^9 s MPa m^{-3}; Tyerman et al. 2004; approx. 5×10^9 s MPa m^{-3}; Choat et al. 2009) were obtained (2.5×10^9 s MPa m^{-3}; Brüggenwirth, unpublished data).

Longitudinal and temporal variation of conductivity and the effect of temperature

The conductivity of the distal end of the pedicel (torus) was lower than of the rest of the pedicel (Fig. 5). Two explanations may be offered. First, the vascular vessels may narrow in the distal part of the pedicel causing a lower conductivity and hence, a bottleneck in the torus (Drazeta et al. 2004). Second, the distal pedicel end merges into the receptacle where the abscission zones of sepals, petals and stamina are present. Those xylem vessels, that branch in the torus region (Brüggenwirth unpublished microscopic observations) and supply the flower organs during anthesis, may become non-functional post-anthesis. Thus, only the vascular vessels feeding the fruit remain functional, whereas closer to the proximal end of the pedicel, more of the vessels (i.e. those serving the fruit plus the flower remnants) are functional, leading to a higher conductivity.

Conductance decreases slightly during development indicating that some xylem vessels may have impaired functionality (Fig. 6). The reason for this partial or complete loss of functionality is unknown. The resulting decrease in flow (for a particular driving force) is consistent with the literature data reporting decreased xylem flows as fruits mature (for apple Lang 1990; Lang and Ryan 1994, for grape Tyerman et al. 2004; Choat et al. 2009; for kiwifruit Morandi et al. 2010; Mazzeo et al. 2013).

The lack of an effect of temperature on flow rate and pedicel conductance was unexpected and somewhat surprising. Because the viscosity of water decreases as temperature increases (Nobel 1999), we would expect the conductance to nearly double with a rise of temperature from 10 to 35 °C. The reason for this apparent discrepancy is not understood.

Conclusions

Using a pressure probe and the protocol described herein, it is possible to measure the axial conductance of the xylem in a sweet cherry fruit pedicel in a satisfactorily reproducible manner. The axial flow recorded essentially follows the Hagen–Poiseuille law, though the experimentally determined conductances and flows are consistently lower than the predicted values. This is likely accounted for by an overestimation of functional cross-sectional areas of the xylem vessels based on microscopical inspections of cross-sections. The only observation we cannot account for is the apparent lack of an effect of temperature.

Conductance estimates are useful for predicting xylem flow rates provided that the driving pressure gradient is known (pedicel length and pressure difference). Using the procedure described herein, future investigations can now focus on resistances in the further portion of the xylem within the flesh of the fruit itself. Such information combined with data on the hydraulic architecture of the tree (Peschiutta et al. 2013) would be useful to fully understand sweet cherry fruit water relations and to clarify the mechanistic basis of fruit cracking.

References

Athoo TO, Winkler A, Knoche M (2015) Pedicel transpiration in sweet cherry fruit: mechanisms, pathways, factors. J Am Soc Hort Sci 140:136–143

Beyer M, Knoche M (2002) Studies on water transport through the sweet cherry fruit surface: V. Conductance for water uptake. J Am Soc Hort Sci 127:325–333

Beyer M, Peschel S, Knoche M, Knörgen M (2002) Studies on water transport through the sweet cherry fruit surface: IV. Regions of preferential uptake. HortScience 37:637–641

Beyer M, Lau S, Knoche M (2005) Studies on water transport through the sweet cherry fruit surface: IX. Comparing permeability in water uptake and transpiration. Planta 220:474–485

Choat B, Gambetta GA, Shackel KA, Matthews MA (2009) Vascular function in grape berries across development and its relevance to apparent hydraulic isolation. Plant Physiol 151:1677–1687

Christensen JV (1996) Rain-induced cracking of sweet cherries. Its causes and prevention. In: Webster AD, Looney NE (eds) cherries. CAB Intl, Wallingford, pp 297–327

Clearwater MJ, Luo Z, Chye Ong SE, Blattmann P, Thorp TG (2012) Vascular functioning and the water balance of ripening kiwifruit (*Actinidia chinensis*) berries. J Exp Bot 63:1835–1847

Drazeta L, Lang A, Hall AJ, Volz RK, Jameson PE (2004) Causes and effects of changes in xylem functionality in apple fruit. Ann Bot 93:275–282

Hovland KL, Sekse L (2004a) Water uptake through sweet cherry (*Prunus avium* L.) fruit pedicels: influence of fruit surface water status and intact fruit skin. Acta Agric Scand Section B-Soil Plant Sci 54:91–96

Hovland KL, Sekse L (2004b) Water uptake through sweet cherry (*Prunus avium* L.) fruit pedicels in relation to fruit development. Acta Agric Scand Section B-Soil Plant Sci 54:264–266

Knoche M, Peschel S, Hinz M, Bukovac M (2000) Studies on water transport through the sweet cherry fruit surface: characterizing conductance of the cuticular membrane using pericarp segments. Planta 212:127–135

Knoche M, Peschel S, Hinz M, Bukovac M (2001) Studies on water transport through the sweet cherry fruit surface: conductance of the cuticle in relation to fruit development. Planta 213:927–936

Knoche M, Athoo TO, Winkler A, Brüggenwirth M (2015) Postharvest osmotic dehydration of pedicels of sweet cherry fruit. Postharvest Biol Technol 108:86–90

Lang A (1990) Xylem, phloem and transpiration flows in developing apple fruits. J Exp Bot 41:645–651

Lang A, Ryan KG (1994) Vascular development and sap flow in apple pedicels. Ann Bot 74:381–388

Mazzeo M, Dichio B, Clearwater MJ, Montanaro G, Xilioyannis C (2013) Hydraulic resistance of developing *Actinidia* fruit. Ann Bot 112:197–205

Measham PF, Bound SA, Gracie AJ, Wilson SJ (2010) Vascular flow of water induces side cracking in sweet cherry (*Prunus avium* L.). Adv Hort Sci 24:243–248

Morandi B, Manfrini L, Losciale P, Zibordi M, Corelli Grappadelli L (2010) Changes in vascular and transpiration flows affect the seasonal and daily growth of Kiwifruit (*Actinidia deliciosa*) berry. Ann Bot 105:913–923

Nobel PS (1999) Physicochemical and environmental plant physiology, 2nd edn. Academic Press, San Diego

Peschel S, Beyer M, Knoche M (2003) Surface characteristics of sweet cherry fruit: stomata-number, distribution, functionality and surface wetting. Sci Hort 97:265–278

Peschiutta ML, Bucci SJ, Scholz FG, Kowal FR, Goldstein G (2013) Leaf and stem hydraulic traits in relation to growth, water use and fruit yield in *Prunus avium* L. cultivars. Trees 27:1559–1569

Sperry JS, Donnelly JR, Tyree MT (1988) A method for measuring hydraulic conductivity and embolism in xylem. Plant Cell Environ 11:35–40

Sperry JS, Hacke UG, Wheeler JK (2005) Comparative analysis of end wall resistivity in xylem conduits. Plant Cell Environ 28:456–465

Steudle E (1993) Pressure probe techniques: basic principles and application to studies of water and solute relations at the cell, tissue and organ level. In: Smith JAC, Griffiths H (eds) Water deficits: plant responses from cell to community. Bios Scientific, Oxford, pp 5–36

Tyerman SD, Tilbrook J, Pardo C, Kotula L, Sullivan W, Steudle E (2004) Direct measurements of hydraulic properties in developing berries of *Vitis vinifera* L. cv. Shiraz and Chardonnay. Aust J Grape Wine Res 10:170–181

Weichert H, Knoche M (2006) Studies on water transport through the sweet cherry fruit surface. 10. Evidence for polar pathways across the exocarp. J Agric Food Chem 54:3951–3958